

Dynamic critical behavior of failure and plastic deformation in the random fiber bundle modelS. Pradhan,* P. Bhattacharyya,[†] and B. K. Chakrabarti[‡]*Saha Institute of Nuclear Physics, 1/AF Bidhan Nagar, Kolkata 700 064, India*

(Received 8 February 2002; revised manuscript received 3 April 2002; published 23 July 2002)

The random fiber bundle (RFB) model, with the strength of the fibers distributed uniformly within a finite interval, is studied under the assumption of global load sharing among all unbroken fibers of the bundle. At any fixed value of the applied stress σ (load per fiber initially present in the bundle), the fraction $U_t(\sigma)$ of fibers that remain unbroken at successive time steps t is shown to follow simple recurrence relations. The model is found to have stable fixed point $U^*(\sigma)$ for applied stress in the range $0 \leq \sigma \leq \sigma_c$, beyond which total failure of the bundle takes place discontinuously [abruptly from $U^*(\sigma_c)$ to 0]. The dynamic critical behavior near this σ_c has been studied for this model analyzing the recurrence relations. We also investigated the finite size scaling behavior near σ_c . At the critical point $\sigma = \sigma_c$, one finds strict power law decay (with time t) of the fraction of unbroken fibers $U_t(\sigma_c)$ (as $t \rightarrow \infty$). The avalanche size distribution for this mean-field dynamics of failure at $\sigma < \sigma_c$ has been studied. The elastic response of the RFB model has also been studied analytically for a specific probability distribution of fiber strengths, where the bundle shows plastic behavior before complete failure, following an initial linear response.

DOI: 10.1103/PhysRevE.66.016116

PACS number(s): 62.20.Mk, 05.50.+q, 05.70.Ln, 05.65.+b

I. INTRODUCTION

A typical relaxational dynamics has been observed in a strained random fiber bundle (RFB) model [1–8] where N fibers are connected in parallel to each other and clamped at their two ends and the strength of the individual fibers has some particular distribution (white, Gaussian, or otherwise). In the global load-sharing approximation [1,2], at any instant, the surviving fibers all share equally the external load (irrespective of their proximity etc. of the fiber to failed fibers etc.). Initially, after the load F is applied on the bundle, a fraction of the fibers having strength less than the applied stress $\sigma = F/N$ fail immediately. After this, the total load on the bundle redistributes globally as the stress is transferred from broken fibers to the remaining unbroken ones. This redistribution causes secondary failures which in general causes further failures and so on. After some relaxation time τ , which depends on σ , the system ultimately becomes stable if the applied stress σ is less than or equal to a critical value σ_c , and beyond which ($\sigma > \sigma_c$) all the fibers break and the bundle fails completely. Although the local load sharing might be more realistic, we study here the global load sharing model because of its simplicity. The study of the scaling properties of the dynamics of the fiber bundle model systems is expected to be extremely useful in analyzing the statistics of fracture and breakdown in real materials, including earthquakes [9,10].

In this paper, we report on the critical dynamics of the RFB model in the global load-sharing case, assuming uniform distribution of threshold strength of the fibers (up to a cutoff), in particular at the critical point σ_c . In a previous paper [11], we have solved the dynamics of the model, showing a novel critical behavior as the stress σ approaches a

certain value σ_c ; we had derived there the expressions for the breakdown susceptibility χ and the relaxation time τ under a stress $\sigma < \sigma_c$ and showed that both the quantities diverge following power laws as σ approaches σ_c from below. Here we define an order parameter for the transition from a state of partial failure of the bundle to a state of total failure and also show that at the critical stress σ_c , the dynamics follows a precise and strict power law. From the finite size dependence of σ_c and the order parameter we have identified the correlation length exponent of the system. We have studied the avalanche size statistics in the model as well. Considering a modified (uniform but shifted from the origin) distribution of fiber strengths we have studied analytically the elastic-plastic deformation characteristics [4] of the RFB model.

II. THE MODEL

The RFB model consists of N elastic fibers clamped at two ends (Fig. 1), where the failure stress of the individual fibers are distributed randomly and uniformly in the interval between 0 and 1 (white or uniform distribution; Fig. 2). Global load sharing is assumed; i.e., the applied load on the bundle is equally shared among all the existing intact fibers. This assumption neglects “local” fluctuations in stress (and its redistribution) and renders the model as a mean-field one. We work with the fraction $U_t \equiv N_t/N$; N_t being the number of fibers remaining intact after t time-steps and $N_{t=0} = N$.

With the application of any small load $F (= \sigma N$, with $\sigma \ll 1$) on the bundle, an initial stress σ (load per fiber) sets in. At this first step therefore, σN number of fibers break, leaving $NU_1(\sigma) = N(1 - \sigma)$ unbroken fibers. After this, the applied force is redistributed uniformly among the remaining intact fibers and the redistributed stress becomes $F/[NU_1(\sigma)] = \sigma/(1 - \sigma)$. Some more fibers, for which the strengths are below the value of the redistributed stress, fail thus leaving $NU_2(\sigma) = N[1 - \sigma/(1 - \sigma)]$ unbroken fibers. This in turn increases the redistributed stress and induces

*Electronic address: spradhan@cmp.saha.ernet.in

[†]Electronic address: pratip@cmp.saha.ernet.in[‡]Electronic address: bikas@cmp.saha.ernet.in

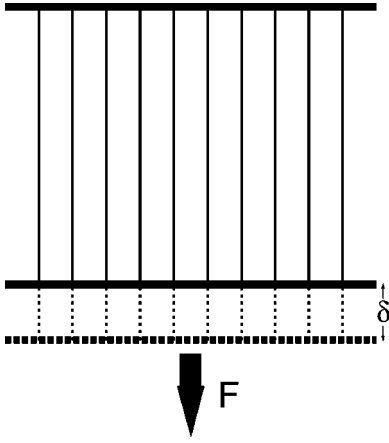


FIG. 1. The RFB model consists of N fibers. The bundle is subjected to a load F . Assuming linear elasticity, with identical elastic constant κ for each fiber up to the breaking, the load F can be expressed as $N\kappa\delta$, where δ denotes the strain for the fibers until any of them breaks. The breaking strengths of the fibers are assumed to be random, as discussed later.

further failures. Consequently, as the stress per fiber $\sigma(t)$ at time t is given by $F/NU_t = \sigma/U_t$ and the surviving fraction is given by $1 - \sigma/U_t$ (see Fig. 2), $U_t(\sigma)$ follows a simple recurrence relation

$$U_{t+1}(\sigma) = 1 - \frac{\sigma}{U_t(\sigma)}. \quad (1)$$

III. BREAKING DYNAMICS OF THE RFB MODEL

The recurrence relation (1) has the form of an iterative map $U_{t+1} = Y(U_t)$. Its fixed point U^* is defined by the relation $U^* = Y(U^*)$ and from Eq. (1) one gets

$$U^*(\sigma) = \frac{1}{2} \pm (\sigma_c - \sigma)^{1/2}, \quad \sigma_c = \frac{1}{4}. \quad (2)$$

The quantity U^* must be real valued as it has a physical meaning: it is the fraction of the original bundle that remains intact under a fixed applied stress σ when the applied stress lies in the range $0 \leq \sigma \leq \sigma_c$. For $\sigma > \sigma_c$ the map does not have a real-valued fixed point and as can be seen from Eq.

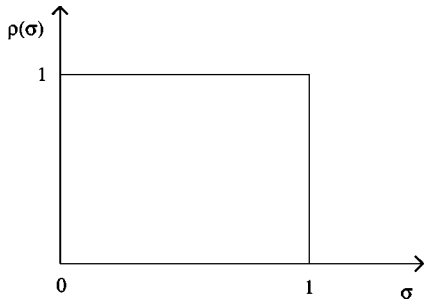


FIG. 2. The simplest model considered here assumes uniformly random distribution or white distribution $\rho(\sigma)$ for the strength of the fibers up to a (normalized) cutoff strength. This distribution gives the recurrence relation (1).

(1), the dynamics never stops until $U_t = 0$ when the bundle breaks completely. Since it requires that $|dY/dU|_{U^*(\sigma)} < 1$ for a fixed point $U^*(\sigma)$ to be stable, for each value of σ the value of U^* with the positive sign in Eq. (2) represents a stable fixed point (or attractor) while the value of U^* with the negative sign in Eq. (2) represents an unstable fixed point (or repeller). It may be noted that the quantity $U^* - 1/2$ behaves like an order parameter that determines a transition from a state of partial failure ($\sigma \leq \sigma_c$) to a state of total failure ($\sigma > \sigma_c$):

$$O \equiv U^* - 1/2 = (\sigma_c - \sigma)^\beta, \quad \beta = \frac{1}{2}. \quad (3)$$

IV. CRITICAL BEHAVIOR

A. For $\sigma < \sigma_c$

To study the dynamics away from criticality ($\sigma \rightarrow \sigma_c$ from below), we replace the recurrence relation (1) by a differential equation

$$-\frac{dU}{dt} = \frac{U^2 - U + \sigma}{U}. \quad (4)$$

Close to the fixed point we write $U_t(\sigma) = U^*(\sigma) + \epsilon$ which, following Eq. (4), gives [11]

$$\epsilon = U_t(\sigma) - U^*(\sigma) \approx \exp(-t/\tau), \quad (5)$$

where $\tau = \frac{1}{2}[\frac{1}{2}(\sigma_c - \sigma)^{-1/2} + 1]$. Approaching σ_c from below we get

$$\tau \propto (\sigma_c - \sigma)^{-\alpha}, \quad \alpha = \frac{1}{2} \quad (6)$$

as the relaxation time of the model and it is found to diverge following a power law as $\sigma \rightarrow \sigma_c$ from below. Although we have used here the continuum-time version (4) of the recurrence relation to evaluate the relaxation time (τ), we have checked numerically as well from the discrete-time recurrence relation (1) and obtained the same exponent value.

One can also consider the breakdown susceptibility χ , defined as the number (fraction) of fibers that break due to an infinitesimal increment of the applied stress [11]

$$\chi = \left| \frac{dU^*(\sigma)}{d\sigma} \right| = \frac{1}{2}(\sigma_c - \sigma)^{-\gamma}, \quad \gamma = \frac{1}{2} \quad (7)$$

from Eq. (2). Hence χ too diverges as the applied stress σ approaches the critical value $\sigma_c = \frac{1}{4}$. Such a divergence in χ had already been observed in the numerical measurements [5,6].

B. At $\sigma = \sigma_c$

At $\sigma = \sigma_c$ the fraction of fibers surviving is $U^*(\sigma_c) = \frac{1}{2}$ and $|dY/dU|_{U^*(\sigma_c)} = 1$ which suggests that the system will take infinite time to reach the fixed point at σ_c . From the recurrence relation (1) it can be shown that this decay of the fraction $U_t(\sigma_c)$ of unbroken fibers that remain intact at time t follows a simple power law:

$$U_t = \frac{1}{2} \left(1 + \frac{1}{t+1} \right), \quad (8)$$

starting from $U_0 = 1$. For large t ($t \rightarrow \infty$), this reduces to $U_t \sim 1/2 \propto t^{-1}$; a simple but strict power law.

V. FINITE SIZE EFFECTS AND CORRELATION LENGTH EXPONENT

For a finite bundle of N fibers, the recurrence relation (1) will be replaced by

$$N_{t+1}(\sigma) = N - \left\lfloor \frac{N^2 \sigma}{N_t} \right\rfloor, \quad (9)$$

where $\lfloor x \rfloor$ denotes the greatest integer less than or equal to x . Here the fixed point is obtained when $N_{t+1} = N_t = N^*$ and the value of N^* is bounded by the relation

$$N \left[\frac{1}{2} + \left(\frac{1}{4} - \sigma \right)^{1/2} \right] \leq N^* < \frac{1}{2}(N+1) + \left[\frac{1}{4}(N+1)^2 - N^2 \sigma \right]^{1/2}, \quad (10)$$

which clearly depends on the finite size of the system. Consequently the effective critical point $\sigma_c(N)$ for the finite RFB model is bounded as

$$\frac{1}{4} \leq \sigma_c(N) < \frac{1}{4} \left[1 + \frac{1}{N} \right]^2. \quad (11)$$

It follows from Eq. (10) that, at $\sigma_c = \frac{1}{4}$, the fixed point value N^* for a finite bundle decays with the initial bundle size N following a power law

$$N_{\sigma_c=1/4}^* \sim \frac{N}{2} \sim N^{1/2}. \quad (12)$$

Since the quantity $U^* - 1/2$ in Eq. (3) behaves like an order parameter for a phase transition, the corresponding quantity in a finite bundle of N fibers would be

$$\frac{N^* - \frac{N}{2}}{N} \equiv U_N^* - \frac{1}{2}. \quad (13)$$

Expressing the correlation length as $\xi \propto (\sigma_c - \sigma)^{-\nu}$ in the infinite system and combining it with Eq. (3) for a finite size system (where $\xi \sim N$), the finite size scaling behavior can be written as

$$U_N^*(\sigma_c) - \frac{1}{2} \sim N^{-\beta/\nu}. \quad (14)$$

Since $\beta = 1/2$, as obtained earlier from Eq. (3), we get $\nu = 1$ by comparing Eq. (14) with Eq. (12).

VI. AVALANCHE SIZE DISTRIBUTION

We now study the avalanche size distribution in this mean-field model. If one considers strictly uniform strength distribution of the fibers in this model, one cannot meaning-

fully approach the failure point by breaking the weakest fiber and looking for the avalanches of successive failures of the fibers, following the avalanche definition of Hemmer *et al.* [2,3]. If we apply this definition in the above (restricted) model, we will end up with only two distinct sizes of avalanches: $(N/2)$ avalanches of unit size and one avalanche of size $(N/2)$. This will occur due to the perfectly uniform strength distribution of the fibers (with the successive strength of fibers differing by $1/N$). To work therefore with a more general definition of avalanche, we increase the external load on the bundle steadily such that the external load F increases by an equal amount ($dF = Nd\sigma$) at each step (cf. [7]). This ensures the bimodal, yet decreasing, distribution function mentioned above to become a smooth (decaying) function. Operationally also, this procedure is quite common and can be applied to different cases and to bundles with different types of strength distribution $\rho(\sigma)$ of fibers. Here, the fraction of fibers m which eventually fail due to this increase in load or stress may be considered as the avalanche size:

$$m = \frac{dM}{d\sigma}; \quad M = 1 - U^*(\sigma). \quad (15)$$

With $U^*(\sigma)$ from Eq. (2) we get

$$\sigma_c - \sigma \sim m^{-2}. \quad (16)$$

If we now define the avalanche size probability distribution by $P(m)$, then $P(m)\Delta m$ measures $\Delta\sigma$, the number of times one has to change σ (by $d\sigma$) to get a change Δm along the m versus σ curve in Eq. (16). In other words,

$$P(m) = \frac{d\sigma}{dm} \sim m^{-\eta}, \quad \eta = 3. \quad (17)$$

This mean-field result for $P(m)$ (power law decay with exponent $\eta = 3$) is obtained here for global load sharing and uniform fiber strength distribution when the external load is increased by a fixed amount. We have checked this result numerically for different $d\sigma$ values ($= 1/N$) for bundles with 50 000 fibers having both strictly uniform and uniform-on-average strength distributions. The results are shown in Fig. 3. The earlier numerical results of Moreno *et al.* [7] for Weibull type distribution of fiber strength also confirms the relation (16), which implies that the cumulative distribution decreases with avalanche size m as m^{-2} , in agreement with Eq. (17).

This result (17) for the avalanche size distribution $P(m)$ is therefore valid for other distributions of fiber strength (cf. [7]) when the avalanche size is defined through Eq. (15). If one looks for the statistics of avalanches initiated by breaking the next weakest fiber in bundles with uniform-on-average fiber strength distribution, as in Hemmer *et al.* [2,3], then one gets $\eta = 5/2$. This is shown in the inset of Fig. 3, where the avalanches are defined in both ways: with fixed increase in σ (giving $\eta = 3.0$) and by breaking the next weakest fiber (giving $\eta = 2.5$). The difference in the above exponent values therefore originates from different ways of

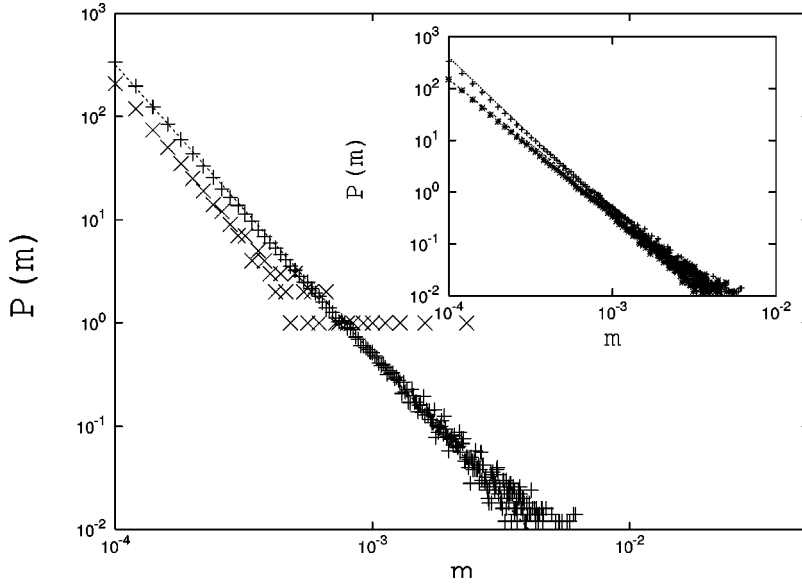


FIG. 3. The log-log plot of the average avalanche size distributions $P(m)$ against m for $N=50\,000$ with $d\sigma=1/N$ for strictly uniform fiber strength distribution (cross) and uniform-on-average fiber strength distribution (averaged over 501 bundle realizations; plus). The dotted line has a slope $\eta=-3.0$, representing Eq. (17). The inset shows the avalanche size distributions for uniform-on-average fiber strength distribution, when (a) the external load increases by a fixed amount $d\sigma=1/N$ (plus) and (b) the avalanches are triggered by breaking the next weakest fiber (star). The dotted and dashed lines in the inset correspond to $\eta=-3.0$ and $\eta=-2.5$, respectively.

defining the avalanches; in our method of defining avalanches here, the external load on the bundle increases uniformly, while in the other method the external load increase has intrinsic fluctuations due to the randomness of the fiber strengths and the restriction on initiating the avalanches by breaking only the next weakest fiber.

VII. PLASTIC DEFORMATION AND STRESS-STRAIN RELATION

One can now consider a slightly modified strength distribution of such a fiber bundle, showing plastic-deformation characteristics [1,4]. For this, we consider a RFB strength distribution, having a lower cutoff. Until failure of any of the fibers (due to this lower cutoff), the bundle shows linear elastic behavior. As soon as the fibers start failing, the stress-strain relationship becomes nonlinear. The dynamic critical behavior remains essentially the same and the static (fixed point) behavior shows elastic-plastic deformation before rupture of the bundle.

Here the fibers are elastic in nature having identical force constant κ (see Fig. 1) and the random fiber strengths distributed uniformly in the interval $[\sigma_L, 1]$ with $\sigma_L > 0$; the normalized distribution of the threshold stress of the fibers thus has the form (see Fig. 4):

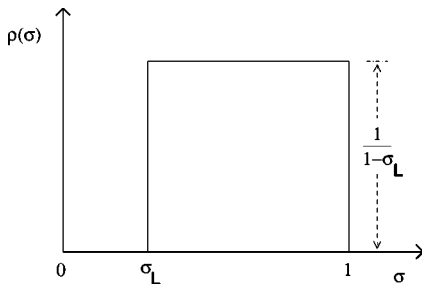


FIG. 4. The fiber breaking strength distribution $\rho(\sigma)$ considered for studying elastic-plastic deformation behavior of the RFB model. This distribution gives the recurrence relation (19).

$$\rho(\sigma) = \begin{cases} 0, & 0 \leq \sigma \leq \sigma_L \\ \frac{1}{1-\sigma_L}, & \sigma_L < \sigma \leq 1 \end{cases}. \quad (18)$$

For an applied stress $\sigma \leq \sigma_L$ none of the fibers break, though they are elongated by an amount $\delta = \sigma/\kappa$. The dynamics of breaking starts when applied stress σ becomes greater than σ_L . Now, for $\sigma > \sigma_L$ the fraction of unbroken fibers follows a recurrence relation [for $\rho(\sigma)$ as in Fig. 4]:

$$\begin{aligned} U_{i+1}(\sigma) &= 1 - \left[\frac{F}{NU_i(\sigma)} - \sigma_L \right] \frac{1}{1-\sigma_L} \\ &= \frac{1}{1-\sigma_L} \left[1 - \frac{\sigma}{U_i(\sigma)} \right], \end{aligned} \quad (19)$$

which has stable fixed points:

$$\begin{aligned} U^*(\sigma) &= \frac{1}{2(1-\sigma_L)} \left[1 + \left(1 - \frac{\sigma}{\sigma_c} \right)^{1/2} \right], \\ \sigma_c &= \frac{1}{4(1-\sigma_L)}. \end{aligned} \quad (20)$$

The RFB model now has a critical point $\sigma_c = 1/[4(1-\sigma_L)]$ beyond which total failure of the bundle takes place. The above equation also requires that $\sigma_L \leq 1/2$ (to keep the fraction $U^* \leq 1$). As one can easily see, the dynamics of $U_i(\sigma)$ for $\sigma < \sigma_c$ and also at $\sigma = \sigma_c$ remains the same as discussed in the earlier section. At each fixed point there will be an equilibrium elongation $\delta(\sigma)$ and a corresponding stress $S = U^* \kappa \delta(\sigma)$ develops in the system (bundle). This $\delta(\sigma)$ can be easily expressed in terms of $U^*(\sigma)$. This requires the evaluation of σ^* , the internal stress per fiber developed at the fixed point, corresponding to the initial (external) stress σ ($=F/N$) per fiber applied on the bundle when all the fibers were intact. From the first part of Eq. (19), one then gets (for $\sigma > \sigma_L$)

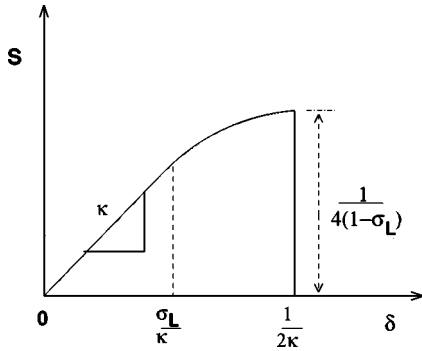


FIG. 5. Schematic stress (S)-strain (δ) curve of the bundle (shown by the solid line), following Eq. (23), with the fiber strength distribution (18) (as shown in Fig. 4).

$$U^*(\sigma) = 1 - \frac{\sigma^* - \sigma_L}{(1 - \sigma_L)} = \frac{1 - \sigma^*}{1 - \sigma_L}. \quad (21)$$

Consequently,

$$\kappa \delta(\sigma) = \sigma^* = 1 - U^*(1 - \sigma_L). \quad (22)$$

It may be noted that the internal stress σ_c^* is universally equal to $1/2$ (independent of σ_L) at the failure point $\sigma = \sigma_c$ of the bundle. This finally gives the stress-strain relation for the RFB model:

$$S = \begin{cases} \kappa \delta, & 0 \leq \sigma \leq \sigma_L \\ \kappa \delta(1 - \kappa \delta)/(1 - \sigma_L), & \sigma_L \leq \sigma \leq \sigma_c \\ 0, & \sigma > \sigma_c \end{cases}. \quad (23)$$

This stress-strain relation is schematically shown in Fig. 5, where the initial linear region has slope κ (the force constant of each fiber). This Hooke's region for stress S continues up to the strain value $\delta = \sigma_L/\kappa$, until which no fibers break [$U^*(\sigma) = 1$]. After this, nonlinearity appears due to the failure of a few of the fibers and the consequent decrease of $U^*(\sigma)$ (from unity). It finally drops to zero discontinuously by an amount $\sigma_c^* U^*(\sigma_c) = 1/[4(1 - \sigma_L)] = \sigma_c$ at the breaking point $\sigma = \sigma_c$ or $\delta = \sigma_c^*/\kappa = 1/2\kappa$ for the bundle. This indicates that the stress drop at the final failure point of the bundle is related to the extent (σ_L) of the linear region of the stress-strain curve of the same bundle.

Here, the plasticity (nonlinearity) in the response of the bundle comes naturally from partial failure of the fibers (and the consequent redistribution of stress among the surviving fibers), after the assumed linear region until the lower threshold σ_L of failure (18). The total failure of the bundle is again

discontinuous here and the entire nonlinear response characteristics are analytically calculable in this simple model.

VIII. SUMMARY AND CONCLUSIONS

We have reported here an analytic study of the failure dynamics and the consequent plastic deformation characteristics of the random fiber bundle model having the property of global load sharing. This has been done here for uniform strength distribution $\rho(\sigma)$ of fibers in the bundle (up to a cutoff). As mentioned before, this has been possible due to the inherent mean-field nature of the model. The recurrence relation (1) captures essentially all the intriguing features of the dynamics. We found that both the breakdown susceptibility χ and the relaxation time τ diverge as the applied stress σ approaches its global failure point σ_c ($= 1/4$ for the uniform strength distribution as shown in Fig. 2) from below, with the same exponent value $\gamma = \alpha = 1/2$. The critical dynamics of the model follows a strict power law decay at $\sigma = \sigma_c$: $U_t - 1/2 \propto t^{-1}$. Though we have identified $O \equiv U^*(\sigma) - 1/2$ as the order parameter (with exponent $\beta = 1/2$) for the continuous transition in the model, unlike conventional phase transitions it does not have a real-valued existence for $\sigma > \sigma_c$. From finite-size scaling study, we see that there is a correlation length which diverges with an exponent $\nu = 1$, as σ_c is approached from below. The avalanche size distribution $P(m)$ for this mean-field dynamics of the RFB model is given by $P(m) \sim m^{-\eta}$, $\eta = 3$. This has been confirmed here numerically. As mentioned before, this result is valid for the avalanche sizes defined through Eq. (16), where the external load on the bundle increases uniformly until the total failure at σ_c . The present as well as the earlier numerical results [5,7,11] all confirm that the analytic results for the exponents α , γ , and η [for τ , χ , and $P(m)$, respectively] are not necessarily restricted to the uniform distribution of fiber strength (assumed here) and are more generally valid. The model also shows realistic plastic deformation behavior with a shifted (by σ_L , away from the origin) uniform distribution of fiber strengths. The stress-strain curve for the model clearly shows three different regions: an elastic or linear part (Hooke's region) when none of the fibers break [$U^*(\sigma) = 1$], a plastic or nonlinear part due to the successive failure of the fibers [$U^*(\sigma) < 1$], and then finally the stress drops suddenly [due to the discontinuous drop in the fraction of surviving fibers from $U^*(\sigma_c)$ to zero] at the bundle failure point at $\sigma = \sigma_c$ [$= 1/[4(1 - \sigma_L)]$ for the failure strength distribution (18)]. Simplicity of the model and consequently of the recurrence relation for the breaking dynamics allows it to have exact analytic results for all its static and dynamic behaviors of breaking and the resulting plasticity.

- [1] H.E. Daniels, Proc. R. Soc. London, Ser. A **183**, 405 (1945).
 [2] P.C. Hemmer and A. Hansen, J. Appl. Mech. **59**, 909 (1992);
 A. Hansen and P.C. Hemmer, Phys. Lett. A **184**, 394 (1994);
 M. Kloster, A. Hansen, and P.C. Hemmer, Phys. Rev. E **56**,
 2615 (1997).
 [3] D. Sornette, J. Phys. I **2**, 2089 (1992).

- [4] D. Sornette, J. Phys. A **22**, L243 (1989); A.T. Bernardes and
 J.G. Moreira, Phys. Rev. B **49**, 15 035 (1994).
 [5] S. Zapperi, P. Ray, H.E. Stanley, and A. Vespignani, Phys. Rev.
 Lett. **78**, 1408 (1997).
 [6] R. da Silveria, Am. J. Phys. **67**, 1177 (1999).
 [7] Y. Moreno, J.B. Gomez and A.F. Pacheco, Phys. Rev. Lett. **85**,

- 2865 (2000).
- [8] R.C. Hidalgo, F. Kun, and H.J. Herrmann, Phys. Rev. E **64**, 066122 (2001).
- [9] B. K. Chakrabarti and L. G. Benguigui, *Statistical Physics of Fracture and Breakdown in Disorder Systems* (Oxford University Press, Oxford, 1997).
- [10] P. Bak, *How Nature Works* (Oxford University Press, Oxford, 1997).
- [11] S. Pradhan and B.K. Chakrabarti, Phys. Rev. E **65**, 016113 (2002).